2009

Self-Organized Ultrathin Oxide Nanocrystals

Ziyang Huo, *University of California - Berkeley*
Chia-Kuang Tsung, *University of California - Berkeley*
Wenyu Huang, *University of California - Berkeley*
Melissa Fardy, *University of California - Berkeley*
Ruoxue Yan, *University of California - Berkeley*, et al.

NANO LETTERS

2009
Vol. 9, No. 3
1260-1264

Self-Organized Ultrathin Oxide Nanocrystals

Ziyang Huo,[†,‡] Chia-Kuang Tsung,[†] Wenyu Huang,[†] Melissa Fardy,[†] Ruoxue Yan,[†] Xiaofeng Zhang,[§] Yadong Li,[‡] and Peidong Yang*[,†]

Department of Chemistry, University of California, Berkeley, California 94720, Materials Sciences Division, Lawrence Berkeley National Laboratory, Berkeley, California 94720, Department of Chemistry, Tsinghua University, Beijing 100084, People's Republic of China, and Nanotechnology Systems Division, Hitachi High Technologies America, Inc., Pleasanton, California 94588

Received January 21, 2009; Revised Manuscript Received January 22, 2009

ABSTRACT

Sub-2-nm (down to one-unit cell) uniform oxide nanocrystals and highly ordered superstructures were obtained in one step using oleylamine and oleic acid as capping and structure directing agents. The cooperative nature of the nanocrystal growth and assembly resulted in mesoscopic one-dimensional ribbon-like superstructures made of these ultrathin nanocrystals. The process reported here is general and can be readily extended to the production of many other transition metal (TiO_2, ZnO, Nb_2O_5) and rare earth oxide (Eu_2O_3, Sm_2O_3, Er_2O_3, Y_2O_3, Tb_2O_3, and Yb_2O_3) systems.

In the past two decades, inorganic colloidal nanocrystals have been intensively investigated due to their broad range of potential applications.[1−4] These nanocrystals[5−10] represent ideal nanoscale building blocks for various nano-enabled devices and systems. A fundamental challenge, however, still remains in the production of uniform ultrathin nanocrystals with sizes of 1−2 nm and down to the one unit cell limit. Here we report a simple process for the synthesis of highly uniform ultrathin oxide nanocrystals. These nanocrystals can have thicknesses as thin as one unit cell of the corresponding crystal lattice. Appropriate surfactants were used in this process both as nanocrystal capping and as structure directing agents. The cooperative nature of the nanocrystal growth and assembly resulted in mesoscopic one-dimensional ribbon-like superstructures made of these ultrathin nanocrystals. The process reported here is general and can be readily extended to the production of many other transition metal and rare earth oxide systems.

Typical nanocrystal studies reported in the literature deal with features of 4−5 nm and above.[11−15] Reports on 1−2 nm nanocrystal syntheses have been rare due to the increased difficulty to control the growth at such an atomic level. TiO_2 nanorods (NRs) are used here as an example to illustrate the effectiveness of our simple method in generating high-quality ultrathin nanostructures and their corresponding self-assembled superstructures. In a typical synthesis, 0.5−0.6 g of titanium isopropoxide or titanium butoxide (reagent grade, 97% from Aldrich) was dissolved in a mixed solvent of dry octadecene (18 g) and oleic acid (16 g) under vigorous stirring at 80 °C for ∼4 h. To this transparent yellow solution, 6−7 g of oleylamine (≥70%, Technical grade from Aldrich) was added and then the entire solution was heated at 260−280 °C under a nitrogen atmosphere. After the reaction was cooled to room temperature, the gel-like product could be readily separated from the bulk solution by centrifugation at 3000 rpm for 10 min (Figure 1a, inset).

Figure 1 shows typical transmission electron microscopy (TEM) images of the as-obtained product at different magnifications. As seen in panels a and b of Figure 1, the product is composed of many well-defined, uniform, ribbon-like structures ∼20 nm in width and ∼600 nm in length. The corresponding energy dispersive X-ray spectroscopy (EDS) analysis (Figure 1b, inset) reveals that the structures contain only oxygen and titanium. Interestingly, upon further increase of the magnification (Figure 1c), it is clear that these ribbon-like structures are actually composed of many ultrathin TiO_2 NRs, ca. 2 nm × 20 nm, which are stacked side-to-side in a highly ordered fashion. High-resolution TEM (HRTEM, Figure 1d) images of these individual building blocks show that the TiO_2 NRs are single crystalline with lattice fringes of 3.50 and 2.38 Å corresponding to the spacings between the (101) and (004) lattice planes, respectively. From this HRTEM study, it can also be concluded that these nanorods grew along the *c* axis. It should be noted here that the self-assembly of these highly uniform ultrathin TiO_2 NRs into oriented ribbon-like superstructures occurred

* Corresponding author, p_yang@berkeley.edu.
[†] University of California, Berkeley, Lawrence Berkeley National Laboratory.
[‡] Tsinghua University.
[§] Hitachi High Technologies America, Inc.

10.1021/nl900209w CCC: $40.75
Published on Web 02/10/2009

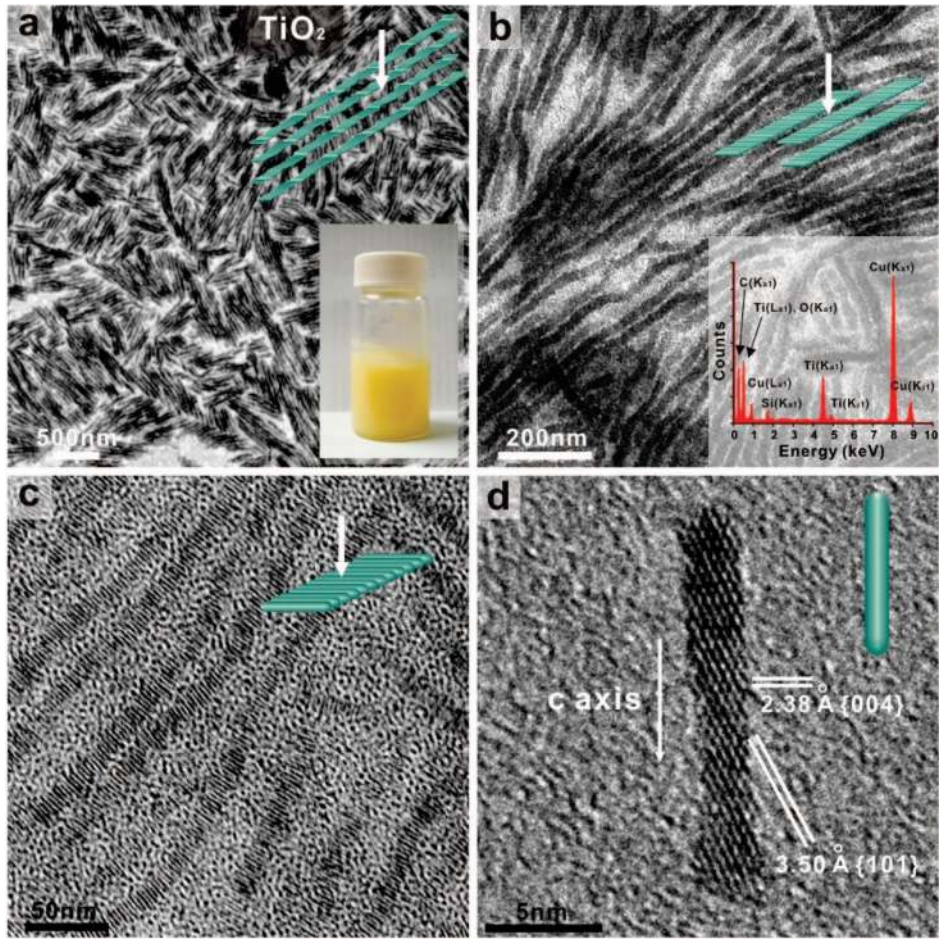

Figure 1. (a−c) TEM images of the as-prepared TiO_2 NRs and their superstructures. Inset in panel a is an image of the as-prepared gel-like product; inset in panel b is the EDS spectrum of the TiO_2 NRs. The copper and silicon signals come from the copper TEM grid and EDS detector, respectively. The carbon signal is present due to the carbon film on the TEM grid and the organic molecules absorbed on the surface of the TiO_2 NRs. (d) HRTEM image of an individual TiO_2 NR.

spontaneously during the initial synthesis of TiO_2 NRs without additional postprocessing steps.

The composition and crystal structure of the reaction products were examined by X-ray diffraction (XRD) at both low and high angles. The high-angle diffraction pattern of the final product (Figure 2) clearly demonstrates that the NRs were composed of pure anatase TiO_2 (JCPDF 21-1272) and that no other crystalline phases or impurities were present. The apparent broadening of the diffraction peaks is indicative of the small size of the TiO_2 nanocrystals. The 004 diffraction peak, on the other hand, exhibits a relatively narrow peak width, which implies the formation of TiO_2 NRs with a preferred growth orientation along the [004], namely, the *c* axis direction of the anatase crystal structure. This is consistent with the HRTEM analysis.

Low-angle XRD was recorded from the gel-like sample after the reaction was aged at 260 °C for 1 h (Figure 1a inset, 2). The XRD pattern shows four well-resolved peaks with *d* spacings of 23.48, 15.73, 11.84, and 9.52 Å, which could be readily indexed to the 00*l* reflection series for a layered mesostructure with layer spacing of ca. 47.2 Å. This 4.7 nm value corresponds well with the thickness of the long chain alkyl molecule bilayer plus the width of the TiO_2 nanorods.[16,17] This low-angle diffraction clearly suggests that

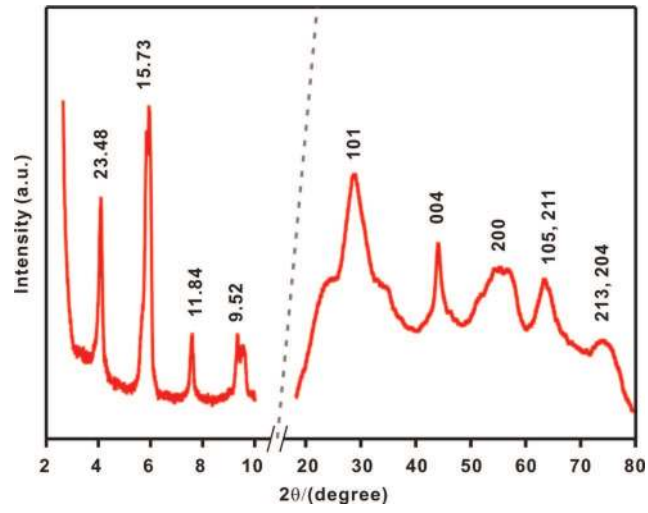

Figure 2. Low-angle and high-angle XRD pattern of the TiO_2−surfactant mesostructures and the final TiO_2 nanorods. Peak labels indicate the corresponding *d* spacings in Å (for low angle) and diffraction index (for high angle).

mesoscopic ordering of the nanorods[18] could occur spontaneously during the synthetic process.

On the basis of these TEM and XRD experimental observations, a cooperative[19,20] nanocrystal growth and self-

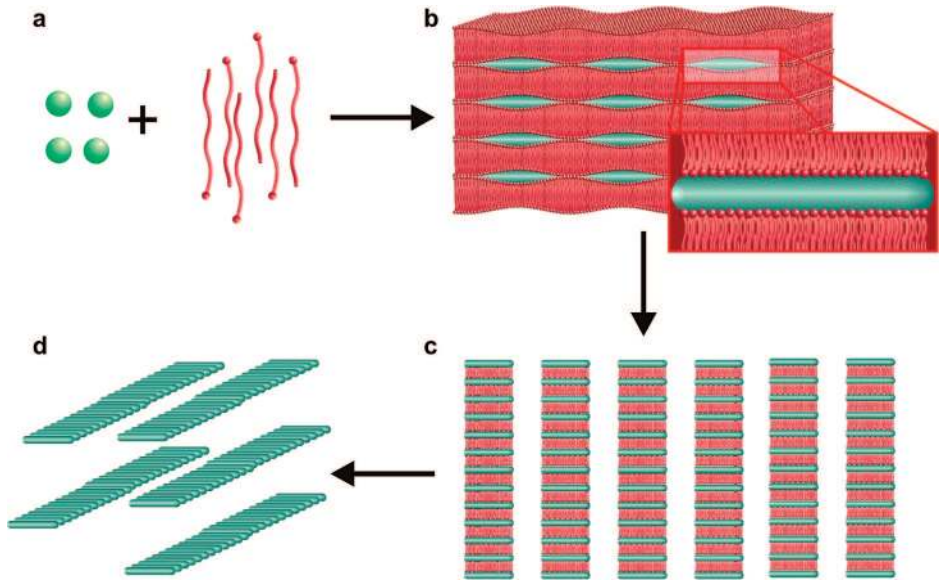

Figure 3. Schematic illustration for the synthesis of ultrathin nanostructures and their assembly.

assembly mechanism is hypothesized (Figure 3). First, inorganic precursor species were complexed with surfactants to form metal−surfactant complex monomers. These complex monomers and excess surfactants were organized into layered mesostructures (Figure 3b, also see Supporting Information for an example of low-angle XRD pattern for the initial layered mesostructures) which contained many nanoscale reactive pockets for oxide nanocrystals to nucleate and grow. The inorganic portion of the monomers was largely restricted in the hydrophilic reactive pockets, and the metal−surfactant complexes were decomposed in situ at high temperature to produce a metal−oxygen network through an ester elimination process.[15,21] After the reaction was heated at a given temperature for several hours, crystalline NRs evolved from the layered mesostructures. The layered mesostructures was then disrupted, and the nanorods spontaneously self-assembled into 1D superstructures (Figure 3c,d). This type of ribbon-like 1D superstructure ensures the largest side-to-side contact area between the nanorods and therefore effectively decreases the interfacial energy.[18,22]

To test this cooperative growth/assembly hypothesis, this synthetic method was applied to a number of other metal oxides. Significantly, many other transition metal oxide nanostructures were prepared with a sub-2-nm dimension. A majority of these oxide nanocrystals spontaneously formed ribbon-like mesoscopic superstructures. For example, panels a and b of Figure 4 show as-synthesized Nb_2O_5 NRs with diameters of 1.3−1.6 nm. Again, these uniform NRs self-assembled into ribbon-like superstructures. XRD and HR-TEM studies confirmed the single crystalline nature of these Nb_2O_5 NRs (Supporting Information, Figure S1,a−d).

Additionally, uniform ZnO NRs of 1.1−1.4 nm in width could be readily generated from ordinary acetate precursors using this simple strategy. There was an earlier report on the synthesis of ZnO quantum rods, but with diameters of 2.2 nm.[23] Panels c and d of Figure 4 show typical TEM images of ZnO NRs and their ribbon-like superstructures at different magnifications. The side-to-side assembled superstructures can have lengths up to ∼1.6 μm with aspect ratios of ∼80.

Apart from the ultrathin nanorods, uniform disklike nanostructured oxides with thicknesses on the order of a single unit cell were also prepared using the same method. Figures 4e and f show as-obtained Eu_2O_3 nanodisks with thicknesses of 1.2−1.4 nm, which is close to its cubic lattice constant of 10.868 Å. These rectangular nanodisks with 20−30 nm in length of a side (Supporting Information part II) were packed into 1D superstructures via face-to-face interaction as shown in panels e and f of Figure 4. Again, according to our TEM and XRD studies, these oxide nanocrystals are all single crystalline. Interestingly, this same simple procedure can be readily applied to many other rare earth oxide systems, including Sm_2O_3, Er_2O_3, Y_2O_3, Tb_2O_3, and Yb_2O_3 (Supporting Information parts III and IV). We note that there are several reports of such ultrathin rare earth oxide nanocrystal formation in the literature.[24−26]

In summary, sub-2-nm (down to one unit cell) uniform oxide nanocrystals and highly ordered superstructures were obtained in one step using oleylamine and oleic acid as capping and structure directing agents. Through the interaction between surfactants and inorganic species, well-organized layered mesostructures with arrays of nanoscale reactive pockets could be formed. The nanoscale reactive pockets limited the growth of oxide nanocrystals, leading to mesoscopic ordering in the final assemblies. This simple synthetic strategy could be applicable for the synthesis of many other functional nanocrystals with similar dimensions and down to the strongly quantum confined region that is not easily accessible with previously reported synthetic protocols. Meanwhile, the well-defined assemblies of these building blocks could offer more opportunities for investigating their collective properties, as well as open the door for other technologically important applications.

Acknowledgment. This work was supported by the Office of Basic Science, Department of Energy. We thank Professor

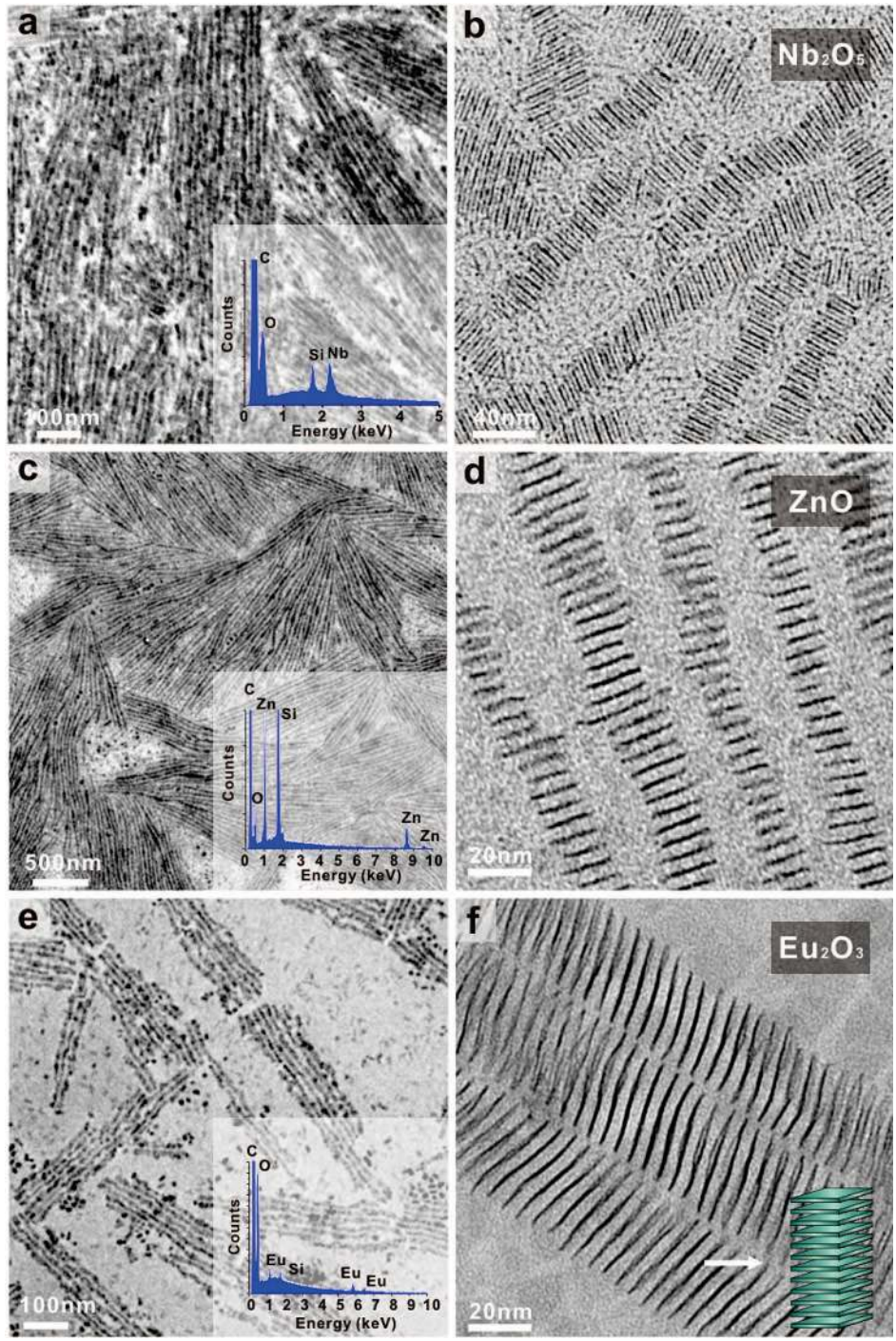

Figure 4. TEM images and the corresponding EDS spectra (inset) of the as-prepared oxide nanocrystals. (a, b) Nb_2O_5 NRs. (c, d) ZnO NRs. (e, f) Eu_2O_3 nanodisks.

A. P. Alivisatos for the use of the TEM and X-ray diffractometer. P.Y. would like to thank NSF for the A.T. Waterman Award. Z.H. would like to thank the Chinese Scholarship Council (CSC) for financial aid.

Supporting Information Available: Description of experimental procedures, XRD patterns and TEM images. This material is available free of charge via the Internet at http://pubs.acs.org.

References

(1) Peng, X. G.; Manna, L.; Yang, W. D.; Wickham, J.; Scher, E.; Kadavanich, A.; Alivisatos, A. P. *Nature* **2000**, *404*, 59–61.
(2) Bruchez, M., Jr.; Moronne, M.; Gin, P.; Weiss, S.; Alivisatos, A. P. *Science* **1998**, *281*, 2013–2016.
(3) Wang, X.; Zhuang, J.; Peng, Q.; Li, Y. *Nature* **2005**, *437*, 121–124.
(4) Mokari, T.; Rothenberg, E.; Popov, I.; Costi, R.; Banin, U. *Science* **2004**, *304*, 1787–1790.
(5) Li, M.; Schnablegger, H.; Mann, S. *Nature* **1999**, *402*, 393–395.
(6) Murray, C. B.; Sun, S. H.; Gaschler, W.; Doyle, H.; Bentley, T. A.; Kagan, C. R. *IBM J. Res. Dev.* **2001**, *45*, 47–56.
(7) Pileni, M. P. *J. Phys. Chem. B* **2001**, *105*, 3358–3371.

(8) Rogach, A. L.; Talapin, D. V.; Shevchenko, E. V.; Kornowski, A.; Haase, M.; Weller, H. *Adv. Funct. Mater.* **2002**, *12*, 653–664.
(9) Huang, J. X.; Kim, F.; Tao, A. R.; Connor, S.; Yang, P. *Nat. Mater.* **2005**, *4*, 896–900.
(10) Tang, Z. Y.; Zhang, Z. L.; Wang, Y.; Glotzer, S. C.; Kotov, N. A. *Science* **2006**, *314*, 274–278.
(11) Chaudret, B. *C. R. Phys.* **2005**, *6*, 117–131.
(12) Burda, C.; Chen, X. B.; Narayanan, R.; El-Sayed, M. A. *Chem. Rev.* **2005**, *105*, 1025–1102.
(13) Jun, Y. W.; Choi, J. S.; Cheon, J. *Angew. Chem., Int. Ed.* **2006**, *45*, 3414–3439.
(14) Cozzoli, P. D.; Pellegrino, T.; Manna, L. *Chem. Soc. Rev.* **2006**, *35*, 1195–1208.
(15) Park, J.; Joo, J.; Kwon, S. G.; Jang, Y.; Hyeon, T. *Angew. Chem., Int. Ed.* **2007**, *46*, 4630–4660.
(16) Messer, B.; Song, J. H.; Huang, M.; Wu, Y. *Adv. Mater.* **2000**, *12*, 1526–1528.
(17) Huo, Z. Y.; Tsung, C. K.; Huang, W. Y.; Zhang, X.; Yang, P. *Nano Lett.* **2008**, *8*, 2041–2044.
(18) Zhang, Z. L.; Horsch, M. A.; Lamm, M. H.; Glotzer, S. C. *Nano Lett.* **2003**, *3*, 1341–1346.
(19) Monnier, A.; Schuth, F.; Huo, Q.; Kumar, D.; Margolese, D.; Maxwell, R. S.; Stucky, G. D.; Krishnamurty, M.; Petroff, P.; Firouzi, A.; Janicke, M.; Chmelka, B. F. *Science* **1993**, *261*, 1299–1303.
(20) Yang, P. D.; Zhao, D. Y.; Margolese, D. I.; Chmelka, B. F.; Stucky, G. D. *Nature* **1998**, *396*, 152–155.
(21) Cozzoli, P. D.; Kornowski, A.; Weller, H. *J. Am. Chem. Soc.* **2003**, *125*, 14539–14548.
(22) Horsch, M. A.; Zhang, Z. L.; Glotzer, S. C. *Phys. Rev. Lett.* **2005**, *95*, 4.
(23) Yin, M.; Gu, Y.; Kuskovsky, I. L.; Andelman, T.; Zhu, Y.; Neumark, G. F.; O'Brien, S. *J. Am. Chem. Soc.* **2004**, *126*, 6206–6207.
(24) Cao, Y. C. *J. Am. Chem. Soc.* **2004**, *126*, 7456–7457.
(25) Si, R.; Zhang, Y.; Zhou, H.; Sun, L.; Yan, C. *Chem. Mater.* **2007**, *19* (1), 18–27.
(26) Yu, T.; Joo, J.; Park, Y.; Hyeon, T. *J. Am. Chem. Soc.* **2006**, *128* (6), 1786–1787.

NL900209W